

Codoping as a measure against donor deactivation in Si: *Ab initio* calculations

D. Christoph Mueller* and Wolfgang Fichtner

Integrated Systems Laboratory, Swiss Federal Institute of Technology, Gloriastrasse 35, CH-8092 Zurich, Switzerland

(Received 22 August 2005; revised manuscript received 9 November 2005; published 19 January 2006)

Based on *ab initio* calculations, we evaluate the effectiveness of various group I, II, and IV elements as possible codopants in highly *n*-doped Si. The fabrication of ultrashallow junctions in future silicon technology requires the suppression of donor deactivation and diffusion during the annealing. The main goal is therefore the elimination of excess vacancies, both isolated and in donor-vacancy (D_nV_m) clusters. We find that the isovalent impurities C and Ge are unsuited for the intended purpose of D_nV_m clustering inhibition. Alkali and earth alkaline metals, on the other hand, can partially reactivate the donors present in clusters at heavy *n*-type doping. Moreover, by annihilating the vacancies, they inhibit in part the vacancy-mediated donor diffusion. Magnesium and beryllium exhibit very promising properties for the codoping strategy proposed in this paper.

DOI: [10.1103/PhysRevB.73.035210](https://doi.org/10.1103/PhysRevB.73.035210)

PACS number(s): 61.72.Ji, 71.15.Mb, 71.20.Mq, 71.55.Cn

I. INTRODUCTION

The ultrashallow junctions in today's silicon devices require dopant concentrations above the respective solid solubility limit of the impurities. In such heavily doped regimes, dopants and intrinsic defects in the crystal begin to interact with one another with deleterious effects on device performance. The pervasive deactivation problem, especially worrisome in arsenic, has been investigated by many researchers, both experimentally and theoretically.¹⁻⁷ Unless new methods are developed, future scaling of transistors will result in a loss of total charge, an increase in sheet resistance and a potential decrease in performance.⁸ Codoping has been considered in compound semiconductors as a possible method to either raise the dopant solid solubility⁹ or to convert dopants exhibiting deep levels into shallow impurities with correspondingly higher activation, i.e., adjust the defect transition energy level.¹⁰ In silicon, codoping has been successfully applied in experiment for the fabrication of ultrashallow *p*-type junctions.¹¹ The main challenge there is to control the concentration of excess interstitials that mediate boron diffusion. In the *n*-type case, however, it is the excess vacancies which are predominantly responsible for both the dopant diffusion (As and Sb) and the electrical deactivation of the donors. Excess vacancies in heavily *n*-doped areas result from implant damage, from Frenkel pair generation, and from indiffusion from the surface due to the abundantly present donor atoms, since at high Fermi levels, the formation energy of negatively charged vacancies decreases correspondingly.¹² These "killer defects" act as powerful acceptors, compensating two, maybe even up to four conduction electrons.¹³ Such vacancies (*V*) are preferably generated in the proximity of one or more donor (*D*) atoms, leading to the well-known D_nV_m clustering.¹⁴ Moreover, the vacancies experience low energetic barriers when traveling between donor atoms in the Si crystal, mediating therefore the very quick dopant diffusion observed in such samples. Codoping in this regime has therefore primarily to aim at annihilating vacancies, both isolated and embedded in donor clusters. The necessity of high doping concentrations and little dopant diffusion implies structures that are far from the thermodynamic equilibrium.

The codopant should therefore act as an anticatalyst, meaning that it should inhibit the rearrangement of donors at annealing temperatures, by occupying the vacant lattice sites necessary for the donor [As, Sb] diffusion and clustering. A potentially effective codopant must therefore meet the following requirements:

- (1) The interstitial codopant should exhibit a large affinity to annihilate a vacancy in a D_nV_m cluster.
- (2) It should introduce negligible extra lattice strain into the crystal, hence small elements are favorable. A moderate diffusivity via interstitial sites is desirable as long as the codopant is trapped at vacancies and D_nV_m clusters.
- (3) The isolated codopant itself should preferably not act as an electron acceptor in any lattice position.
- (4) The codopant should fill up the vacancy electron acceptor states when annihilating a vacancy, transforming the D_nV_m cluster from electron acceptors back into electron donors.
- (5) The codopant should not form clusters that lower the electrical conductance. However, a high codopant solubility in Si is not necessary as long as the precipitation process is not faster than the D_nV_m clustering.

II. SIMULATION SETUP

Our simulations were performed with the density functional theory (DFT) code Vienna *ab initio* simulation package^{15,16} (VASP) with a supercell of $N=216$ atoms. All calculations were carried out in the generalized gradient approximation to the exchange-correlation energy functional and with projector augmented wave pseudopotentials.¹⁷ For the simple metals, the semicore *p* states were treated as valence electrons, as these states tend to relax substantially when the impurities are ionized in the Si crystal. The cutoff energies for the plane-wave-basis sets ranged from 18 Ry to 29 Ry, depending on the elements involved. The *k*-point sampling was done with a 2^3 Monkhorst¹⁸ set. Atomic relaxations were considered until the total supercell energy difference was less than 1 meV. For a charged defect, a uniform background charge is added to keep the global charge neutrality of the periodic supercell. The first order corrections of

the spurious Coulomb interactions between charged defects in different cells tend to be small ($>0.1Q^2$ eV, with Q the defect charge). This value assumes point charges and even overestimates the corrections for shallow (extended) defect states.¹⁰

In the supercell approach, it is inevitable that the calculated defect states, either shallow or deep, show some kind of dispersion. It appears that within the framework of the supercell approach, it is consistent to calculate the *average* one-particle level positions with respect to the *average* band edges. The valence band and conduction band edges are then evaluated at special k points (Monkhorst-Pack) instead of taking the actual valence band maximum for Si at the Γ point and the conduction band minimum (CBM). The well-known underestimation of the fundamental band gap by DFT is then partly compensated for, though in a rather unexpected way. Since the total energy is calculated with a Brillouin zone sum over the special k points, the one-particle levels calculated this way are consistent with the defect transition energy levels calculated from the total energy difference between two different charge states, provided the Frank-Cordon shift is negligible. The ionization levels are calculated by solving for the electron chemical potential μ_e in

$$E_{SC}^Q + Q(E_v^Q + \mu_e) = E_{SC}^{Q'} + Q'(E_v^{Q'} + \mu_e). \quad (1)$$

Here, μ_e gives the position of the Fermi level in the band gap relative to the valence band ϵ_v , E_{SC}^Q represents the total energy of the supercell, containing the defect in charge state Q , and ϵ_v^Q is the position of the valence band edge in the corresponding supercell, respectively. Since all configurations were relaxed, the geometry of a defect may vary slightly for different charge states. Assuming that $\epsilon_v^Q \approx \epsilon_v^{Q'}$, it follows immediately from (1) that the ionization energy $Q \rightarrow Q'$ for the Q -charged defect is

$$\mu_e = \frac{E_{SC}^{Q'} - E_{SC}^Q}{(Q' - Q)} - \epsilon_v^Q. \quad (2)$$

The energy μ_e in Eq. (2) thus has to be interpreted as the Fermi level at which the transition $Q \leftrightarrow Q'$ of the corresponding defect occurs. For the above-mentioned reasons, defect levels calculated in this way have an inherent uncertainty. However, comparison with experimental values in general yields a fair to good agreement.²⁸ Moreover, for the discussion of deactivating and reactivating defects and clusters, it is often crucial to know whether the defect can act as an electron acceptor or donor, while the exact position of the defect levels is of minor importance.

Figures 1 and 2 illustrate binding energies between codopants and various As_nV_1 clusters, calculated with respect to two different reference states. In Fig. 1, the reference states are the *interstitial* codopant and the infinitely separated As_nV_1 cluster ($n=0-4$). Displayed is the gain in energy E_b^{int} when an interstitial codopant (M_i) $^{Q''}$ with charge state Q'' moves onto the vacant lattice site in the $(As_nV_1)^{Q'}$ cluster with charge state Q' , in order to form an $(As_nM_s)^Q$ cluster with charge state Q .²⁹ This binding energy E_b^{int} can, therefore,

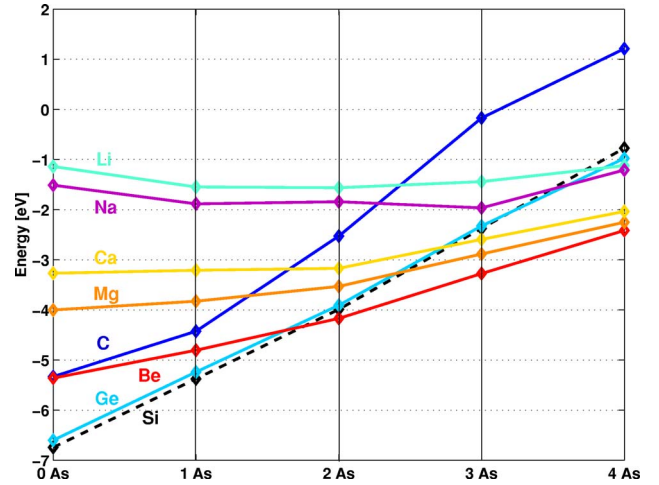


FIG. 1. (Color online) Vacancy trapping energies at high Fermi level: Displayed is the difference in energy of the system when an *interstitial* codopant assumes a formerly vacant lattice site next to 0–4 arsenic atoms, according to Eq. (3). The trapping energy is small for the alkali metals Li and Na because these light metals cause minimal lattice distortion when interstitial.

also be interpreted as a “vacancy trapping energy,” and is calculated as follows:

$$E_b^{\text{int}}(\mu_e) = E(As_nM_s)^Q - E(As_nV_1)^{Q'} - E(M_i)^{Q''} + E(Si)^0 + (Q - Q' - Q'')(E_v + \mu_e), \quad (3)$$

where E is the total energy of the supercell, M_s and M_i denote the codopant in substitutional and interstitial positions, respectively, $E(Si)^0$ is the energy of a neutral supercell containing N Si atoms, and $E(As_nV_1)^{Q'}$ denotes the energy of the supercell containing one As_nV_1 cluster and missing Q' electrons. In this paper, μ_e is assumed to be at the average conduction band edge, reflecting high n doping. The charge

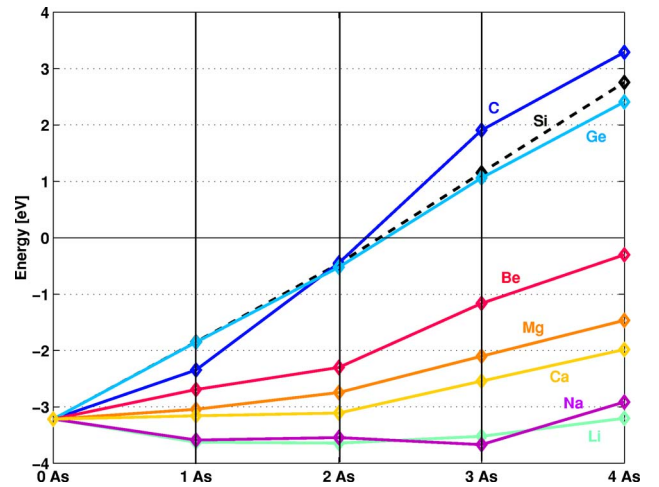


FIG. 2. (Color online) Energy difference for a *substitutional* codopant assuming a formerly vacant lattice position next to 0–4 arsenic atoms, according to Eq. (4). The plot shows that all group I and II codopants form thermodynamically stable complexes with up to four arsenic donors.

states of all defects involved have been evaluated for this high Fermi level according to the defect levels calculated with (2). If the reference state is the *substitutional* codopant, the binding energy E_b^{sub} to an As_nV_1 cluster is given by

$$E_b^{\text{sub}}(\mu_e) = E(\text{As}_n\text{M}_s)^Q - E(\text{As}_n\text{V}_1)^{Q'} - E(\text{M}_s)^{Q''} + E(\text{Si})^0 \frac{N-1}{N} + (Q - Q' - Q'')(E_v + \mu_e). \quad (4)$$

These energies are plotted in Fig. 2. For all codopants, different interstitial configurations were examined, and the lowest in energy were taken as the interstitial reference states:

(1) For the Si self-interstitial, an extensive *ab initio* molecular dynamics analysis at various temperatures determined the split $\langle 110 \rangle$ interstitial state to be the most important. According to our calculations, this defect configuration exhibits two acceptor states in the band gap and is therefore charged -2 at the Fermi level assumed in this paper.

(2) For both isovalent codopants C and Ge, the split interstitial configuration is energetically favored. As in the case of Si, the split interstitials of C and Ge exhibit two in-gap acceptor states.

(3) For the alkali and alkaline earth metals, the tetrahedral configuration (or a configuration in which the codopant is very close to the tetrahedral site) is clearly energetically favored at the defect charge states corresponding to the high Fermi level. Hexagonal interstitial configurations are higher in energy by differences ranging from 0.56 eV (Li) to 1.36 eV (Ca), whereas the split interstitial configurations of Li, Be, and Mg are not even metastable (no local energy minima). The reference charge states are discussed in Sec. V.

III. DEACTIVATION MECHANISMS: THE THREE-STEP MODEL

Based on both the experimental observations and on our extensive *ab initio* studies, we proposed a three-step model of donor deactivation in highly *n*-type silicon,¹⁹ which can be summarized as follows:

(1) At high dopant concentration, even in the absence of dopant diffusion, deactivation is partially due to lattice distortions (δ^3) and the presence of dimers. δ^3 defects can be viewed as precursors to the D_nV_m formation and lower the dopant donor levels deeper in the band gap. These distortions are not a local energy minimum but the entropy term stabilizes them already at moderate temperatures.

(2) The formation of D_nV_m clusters occurs during the first few seconds of annealing.^{5,20} These defects are very efficient at deactivating the donors involved¹³ and can explain the observed loss of activation of up to 90% in samples that have undergone rapid thermal annealing (RTA).

(3) For longer annealing schemes, inactive donor precipitates start to form. They constitute the final annealing stage as the thermodynamic equilibrium is being reached and the solid solubility limitation shows.

As elucidated in Ref. 19, deactivation upon δ^3 defects is inherent to highly *n*-type silicon and is, therefore, not dependent on the concentration of native point defects and, consequently, also independent of the wafer processing method.

TABLE I. Binding energies of donors with the Si lattice vacancy and group IV elements (in meV).

r_{covalent}	P 1.06 Å	As 1.20 Å	Sb 1.40 Å	C 0.77 Å	Ge 1.22 Å
V	-1264	-1395	-1532	-291	-138
C	+283	+157	-67		
Ge	-67	-56	-62		

D_nV_m formation, on the other hand, could be avoided if the clustering process can be forestalled.

IV. ISOVALENT IMPURITIES

With its similar covalent radius and electronic structure with four valence electrons, Ge introduces minimal lattice strain into the silicon lattice as a substitutional impurity, such that the two elements form perfect crystals for various mixing ratios. Carbon is a common impurity in single crystal silicon grown from either the melt or from the vapor phase epitaxy and molecular beam epitaxy. In stark contrast to Ge, interstitial carbon provokes strong lattice relaxations and, therefore, tensile stress in Si. We calculated the inward shift of the next neighboring Si atoms from their perfect lattice positions as 0.35 Å or 14.6% of the Si-Si bond length. However, because of their sp^3 valence structure, neither substitutional C nor Ge introduce defect levels in the Si band gap. Hence, they remain electrically inactive for any position of the Fermi level and will never act as carrier sinks neither in *n*-type nor *p*-type Si as long as they are isolated and substitutional. They could, therefore, theoretically be valuable candidates in the search for a reactivating codopant.

Even though the large As and Sb atoms would prefer a small neighboring atom in the Si crystal due to stress relaxation, electronic repulsion between the donors and the small C results in a slightly positive formation energy, as is also the case for phosphorus (see Table I). Consequently, no significant solubility enhancement for As or Sb can be expected by codoping with C. On the other hand, the larger Ge atom binds—though weakly—with any donor. The reason can be found again in the interaction behavior of the two valence shells. However, the binding energies of donors with a vacancy are about an order of magnitude higher than the corresponding binding energies of group IV elements (see Table I). This fact reflects the relatively high energy cost for the adaptation of the valence shell structure of donors when placed in a tetrahedrally bonded crystal structure.

Interestingly enough, at high Fermi levels, carbon will compensate any donor next to it, as is illustrated by the DFT electron density plot in Fig. 3 for the C-As complex. A charge transfer from the As to the C atom takes place, such that the complex gets polarized and the carbon atom binds the As donor electron. Consequently, the donor level sinks deep into the Si band gap, lying now merely 200 meV above the valence band edge (Fig. 3). The same happens for P and Sb when forming a pair with C, though the deleterious effect is least pronounced for the large Sb atom. Moreover, the

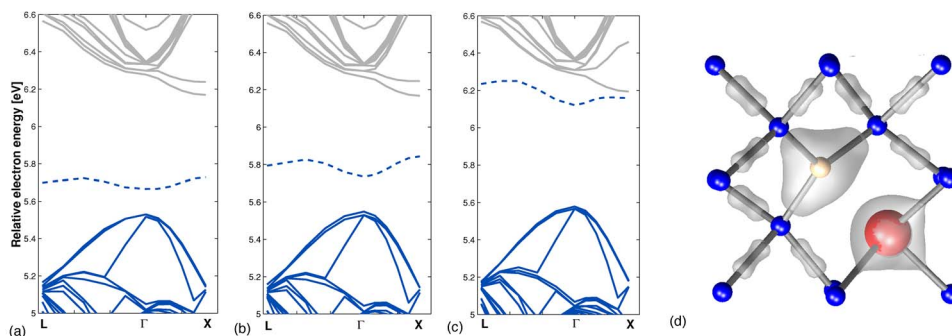


FIG. 3. (Color online) Band structures of donor-carbon pairs. From left to right: (a) C-P pair, (b) C-As pair, (c) C-Sb pair. Full bands are depicted in black, empty bands are gray, and bands occupied by only one electron are represented by dashed lines. For all three donor species, the pairing with carbon has a deactivating effect, as the donor levels sink deep into the band gap. (d) C-As pair in the Si lattice, seen in the $\langle 100 \rangle$ direction: The charge density plot reveals the strongly localized donor state of As, mainly centered around the C atom. The dopant-codopant pair is hence neutral and electrically inactive at high Fermi levels.

C-As pair exhibits a binding energy of +157 meV, reflecting the electronically unfavorable configuration, even though C considerably reduces the lattice strain around the large As atom. Germanium, on the other hand, leaves the donors electrically active (Fig. 4). Nevertheless, there is no significant bonding established between the two impurities, as the charge density plot in Fig. 4 reveals.

As mentioned above, the split interstitial C and Ge are found to have two acceptor states in the band gap. For μ_e at the conduction band edge, the C and Ge interstitials are, therefore, found in charge states -2 . The vacancy trapping energies E_b^{int} for C and Ge, as depicted in Fig. 1, are quite large for 0 or 1 As atom next to the vacancy, because the interstitial codopants, due to their size, are energetically disfavored compared to the substitutional configurations. Hence, the large energy difference when a supposedly interstitial C or Ge gets trapped at a vacancy site. But the numbers E_b^{sub} for C and G in Fig. 2 reveal that the two isovalent impurities will—just like the host atom Si—not form thermodynamically stable clusters close to more than two arsenic donors. The above findings directly imply that both carbon and germanium are unsuited as clustering inhibitors.

V. ALKALI AND EARTH ALKALINE METALS

A. Electric behavior in Si

Light elements of the first and second group in the periodic table tend to donate their weakly bound valence s elec-

trons in the Si crystal, whether on substitutional or in an interstitial lattice site. However, when the dopants reside on substitutional sites, the configuration may be viewed as a Si lattice vacancy occupied by the metal dopant, in order to better understand its electronic structure. Now, the valence s electrons fill up one or two upper T_2 states of the Si lattice vacancy, respectively, making the metals act as acceptors.²¹ This effect can clearly be seen in Fig. 5: The light metals tend to stabilize the four Si dangling bonds that produce the in-gap vacancy states. All of the examined *substitutional* alkali and earth alkaline metals, therefore, act as triple or double acceptors, and a simple rule of thumb for the charge state Q in the n -type regime can be devised

$$Q_{\text{interst.}} = +n_v, \quad (5)$$

$$Q_{\text{substit.}} = +n_v - 4 + N_{\text{As}}, \quad (6)$$

where N_{As} and n_v denote the number of adjacent arsenic atoms and the number of valence electrons of the metal, respectively. The -4 stems from the above-mentioned vacancy acceptor states. Equation (6) immediately implies that isolated, substitutional alkali metals are charged -3 and earth alkalines -2 . The exception to the rule is substitutional Na, which can only bind two extra electrons. The smaller Li, however, indeed appears to adopt a charge state Li^{-3} , which is remarkable in view of the strong Coulomb repulsion of the localized electrons. This in turn means that if these light metals happen to be substitutional, they may become power-

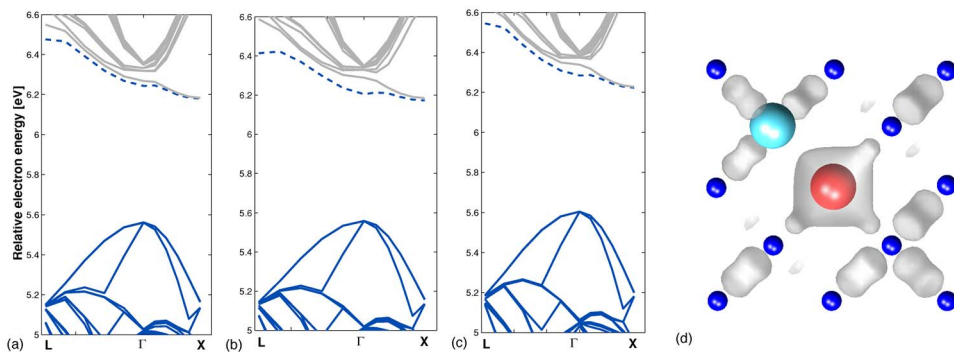


FIG. 4. (Color online) Donor-germanium pairs. From left to right: (a) Ge-P pair, (b) Ge-As pair, (c) Ge-Sb pair. For all three donor species, the pairing with germanium leaves the donor electrically active. (d) The substitutional Ge-As pair in silicon, seen in the $\langle 100 \rangle$ direction (Ge in the upper left, As at the center): Both dopants are threefold bonded.

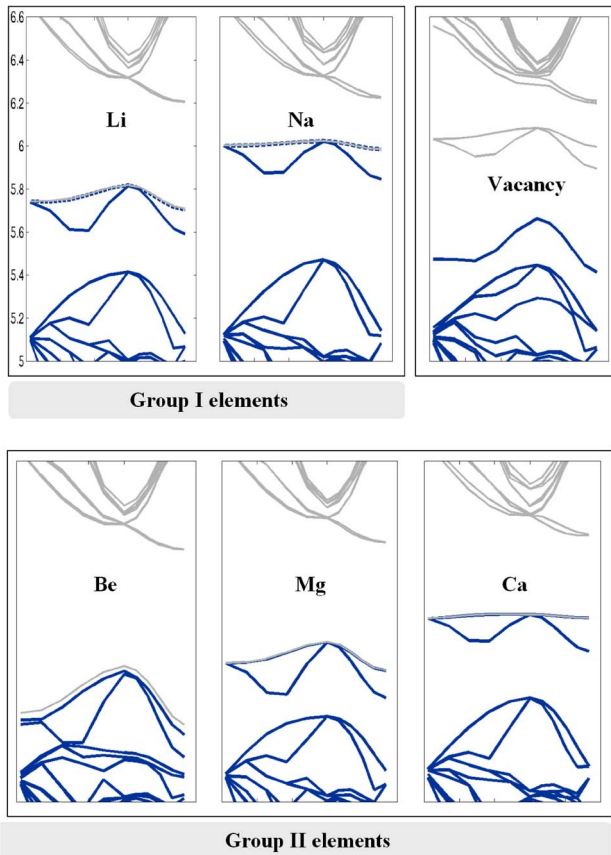


FIG. 5. (Color online) Band structures of simple metals in silicon in substitutional lattice positions: The weakly bound s electrons of the group I/II elements get trapped in the vacancy acceptor states. The configurations then act as electron acceptors. Electron energies are given in eV.

ful electron sinks in the high Fermi level regime. By consequence, neither of these light metals can electrically passivate an isolated Si vacancy completely. Instead, an acceptorlike substitutional metal will result.

In the energetically favored tetrahedral site, on the other hand, the metals exhibit n -type character: As illustrated in Fig. 6, Li and Na exhibit extremely shallow donor levels, merely 7 meV and 10 meV below the CBM respectively. The donor levels of the interstitial double donor earth alkaline metals become shallower with growing atomic number: Interstitial Ca has very weakly bound s states, resulting in a charge +2 state according to (5). For magnesium, a charge state +1 is more likely at very high positions of the Fermi level. And interstitial Be shows yet stronger binding energies of its valence electrons, as the band structure plot (Fig. 6) of interstitial Be with its deep donor levels reveals. At very high Fermi levels, therefore, it remains neutral.

If the vacancy is surrounded by two donors, a metallic codopant can convert the As_2V complex into an electrically neutral As_2M defect. Equation (6) also correctly predicts the electrical behavior of As_3M complexes: For an earth alkaline codopant ($n_v=2$), such a complex acts as a single electron donor (see Fig. 7). If the codopant is an alkali metal with $n_v=1$, the complex will remain electrically neutral. The lo-

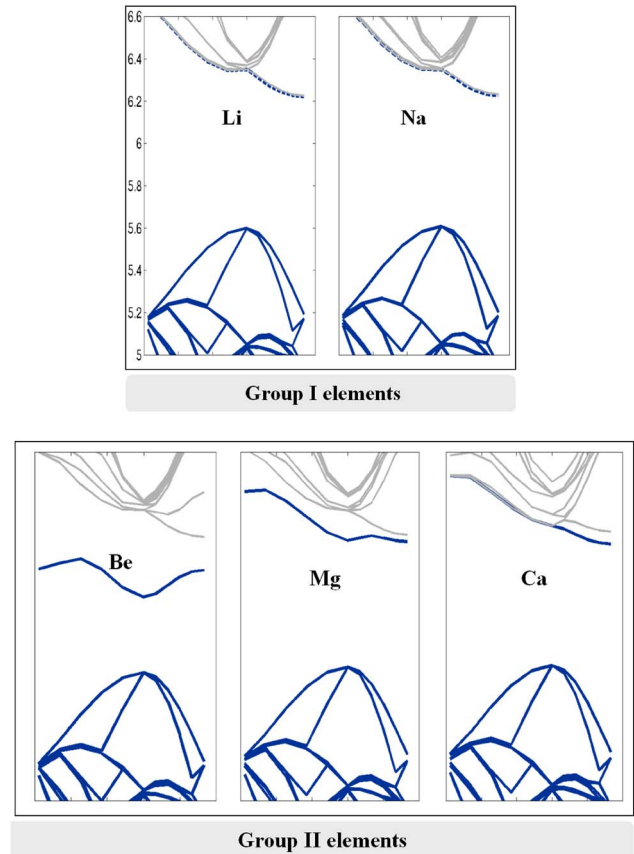


FIG. 6. (Color online) In the tetrahedral interstitial lattice position, all of the light group I/II elements act as donors. The deep donor states of Be, however, make the codopant remain electrically neutral at elevated Fermi levels. Electron energies are given in eV.

cations of the corresponding levels for the group I and II elements are listed in Table II. Hence, an earth alkaline metal will convert the acceptorlike As_3V cluster into a shallow donor As_3M complex. Since the former seems to be the predominant cluster in highly As-doped, thermally annealed samples,²² an arsenic reactivation of up to 50 % can be expected due to As_3M complex formation. In the As_4M clusters, the earth alkalines Be, Mg, and Ca even transform the complex to a double donor.

B. Trapping of codopants at dopant clusters

Besides their ability to neutralize acceptor levels of both V and $D-V$ clusters, the tendency to be trapped at lattice vacancies is a prerequisite of an effective codopant. In addition, the codopant should exhibit a high diffusivity in order to quickly reach the compensating defects, preferably with a diffusion mechanism that is independent of vacancies. Small atoms with little interaction with the Si lattice are, therefore, in general favored. However, a little lattice interaction of a small interstitial codopant also implies a correspondingly small vacancy trapping energy according to Eq. (3), as elucidated in Fig. 1 for the small Li and Na with vacancy trapping energies of 1.14 eV and 1.51 eV, respectively. These atoms move along the $\langle 111 \rangle$ channels in a zigzag fashion,

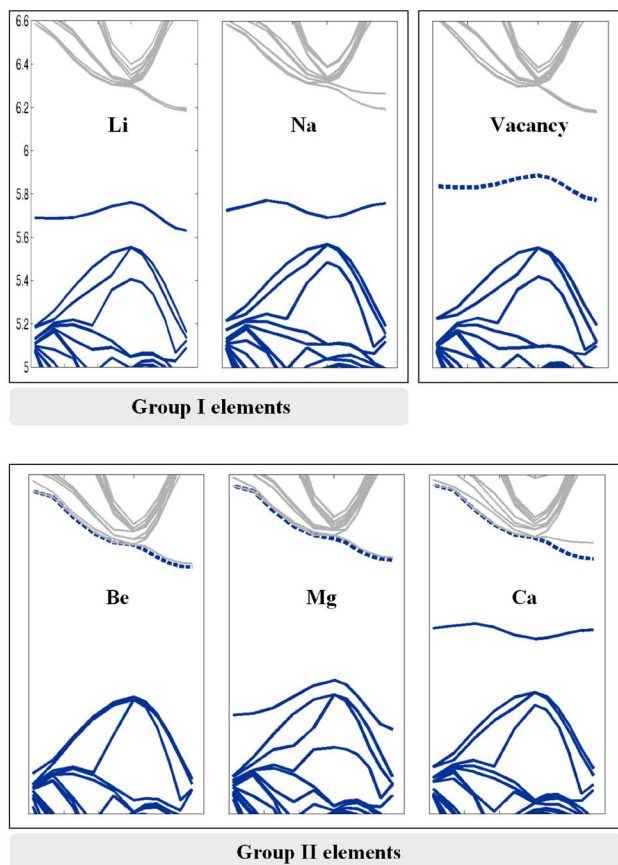


FIG. 7. (Color online) Band structures of simple metals (M) in silicon in the As_3M cluster: While the As_3V was a single electron acceptor, the clusters containing an earth alkaline exhibit a shallow donor level. Electron energies are given in eV.

alternatively passing through the tetrahedral and hexagonal interstitial sites of the lattice, which are their equilibrium and saddle points for diffusion.^{23–25} On the other hand, a high diffusivity of a possible codopant is not desirable in the manufacturing process of shallow junctions. However, experiments have shown that the presence of 10^{18} cm^{-3} carbon reduces the room temperature diffusion rate of Li to 0.1% of its value in pure Si.²⁶ It is therefore very likely that also in heavily n -doped samples, all of the metals discussed exhibit a dramatically reduced diffusivity, due to their tendency to bind to donors and donor-vacancy clusters. The energy difference of the migration process from the interstitial to the substitutional position is small for the alkali metals Li and Na because these light metals cause minimal lattice distortion when interstitial, as mentioned above. Interstitial C, Si, and Ge, on the other hand, evoke large lattice relaxations, such that the substitutional configuration is energetically favored for any number of neighboring As atoms, by up to 6.74 eV.³⁰ The trapping energies of the earth alkaline metals Ca, Mg, and Be are smaller than those of the group IV elements in undoped Si (0 As on the x axis), but at high arsenic doping, an interesting feature becomes apparent: The ionized interstitial earth alkalines, though small, show an even stronger tendency to annihilate vacancies in the As_3V and As_4V complexes than the large Si interstitial. Especially Mg and

TABLE II. Ionization energies of earth alkaline metals in the band gap: Donor (D) and acceptor (A) levels are given in eV with respect to the *averaged* conduction band edge and valence band edge, respectively. The values are evaluated with Eq. (2). Referenced numbers are experimental values. M_s and M_i refer to the codopant in a substitutional and interstitial site, respectively.

Codopant	M_s	M_i (tetrahedral)	As_3M
Li	A_3 0.787	D_1 0.007	D_1 0.780
	A_2 0.625		D_2 0.910
	A_1 0.483		
Na	A_2 0.829	D_1 0.010	D_1 0.724
	A_1 0.708		D_2 0.906
Be	A_2 0.152	D_1 0.340	D_1 0.007
	A_1 0.089	D_2 0.425	
	$(A_1$ 0.17) ^a		
Mg	A_2 0.350	D_1 0.074	D_1 0.001
		$(D_1$ 0.11) ^b	
	A_1 0.282	D_2 0.095	$(D_2$ 0.25) ^b
Ca	A_2 0.696	D_1 0.003	D_1 0.013
	A_1 0.562	D_2 0.012	

^aReference 33.

^bReference 34.

Be are therefore major codopant candidates for the preclusion of rapid donor diffusion and/or percolation and As_3V cluster formation.

Figure 2 summarizes the energy gain of the super cell when a substitutional codopant assumes a formerly vacant lattice position next to 0–4 arsenic atoms. For the isolated vacancy (0 As on the x axis), this energy corresponds to the negative vacancy formation energy in Si for the Fermi level μ_e and is independent of the codopant species. When one or more donors are adjacent to the vacancy, then the discrepancy between group IV elements and light metals becomes apparent. The dashed line for the Si atom illustrates the fact that both As_3V and As_4V are thermodynamically stable complexes: The As_3Si and As_4Si complexes are 1.15 eV and 2.76 eV higher in energy than the configurations with a central vacancy, respectively (μ_e at the conduction band edge). This is not the case for the As_3M and As_4M complexes if the codopant M is an alkali or earth alkaline metal. Hence, in the *absence* of a light metal codopant, the As_3V and As_4V complexes will be formed given enough time and thermal energy to allow the system evolve toward the thermodynamic equilibrium.² But in the presence of light alkali or earth alkaline codopants, the metal codopants will associate with the complexes at a high energy gain of -3.67 eV to -0.31 eV, whereupon the electrical activation of the donors involved is partially restored, as explained above.

C. Codopant clustering

Obviously, the codopants will interact among themselves as well. A possible codopant cluster should, however, not act

TABLE III. Formation energies (in eV) for pairs of earth alkaline metals (M) in various configurations in crystalline Si. Below, the electrical behavior in highly n -type Si is indicated.

	M_s-M_i	$(M-M)_{split}$	As_sM_i	M_i-M_i
Mg	-1.64 (inactive)	-1.27 (inactive)	-0.043 (donor)	-0.105 (donor)
Be	-1.35 (acceptor)	-0.39 (inactive)	-0.074 (donor)	-0.729 (inactive)

as an electron compensator at high Fermi levels. We studied various codopant clusters of the two most promising candidates Mg and Be. The corresponding formation energies, summarized in Table III, are given for μ_e at the conduction band edge and with respect to two infinitely separated impurities, one in a substitutional (M_s) Q and one in an interstitial (M_i) $^{Q'}$ lattice site, with charge states Q and Q' respectively, according to the Fermi level. Formation energies of the M_i-M_i pairs, on the other hand, are given with respect to two infinitely separated interstitial codopants.

The most relevant codopant pair configuration is the $\langle 111 \rangle M_s-M_i$ pair with the two codopants occupying a lattice site and an adjacent tetrahedral interstitial site. In the case of Mg, this configuration exhibits a binding energy of -1.64 eV according to our calculations. Therefore, an interstitially diffusing Mg atom is—with trapping energies ranging from -4.00 eV to -2.25 eV—considerably more attracted to an $As_nV(n=1-4)$ cluster than to a substitutional Mg. Similar figures are found in the case of the Be codopant: The Be-Be $\langle 111 \rangle M_s-M_i$ pair exhibits a binding energy of -1.35 eV, while trapping energies to As_nV clusters are between -5.36 eV to -2.41 eV for $n=0-4$. Both Mg_2 and Be_2 pair formations in heavily n -doped Si should thus be substantially less predominant than earlier simulations in pure Si by Tarnow *et al.* suggested.²⁷ Other possible pair configurations are Mg_2 and Be_2 split interstitials, where the two metal atoms share a common lattice site. These configurations exhibit formation energies of -1.27 eV and -0.39 eV, respectively, and are, therefore, less likely to form than the $\langle 111 \rangle M_s-M_i$ pairs. Furthermore, two interstitial earth alkaline metals only

slightly attract each other. In the energetically most favored configuration of such a M_i-M_i interstitial pair,³¹ the Mg metals bind with 105 meV, whereas two Be interstitials bind with 729 meV. We studied the electronic structure of all of these Mg_2 and Be_2 pairs in bulk Si and found most of them to be either inactive or electron donors at high Fermi levels, as indicated in Table III. Only the Be_s-Be_i pair acts as a single electron acceptor.³² Consequently, the clustering of codopants does not jeopardize the high electron concentration. In fact, the codopant clustering of Mg indeed even further helps to increase the net number of conduction electrons in the bulk.

VI. CONCLUSIONS

We have investigated the isovalent impurities C and Ge, as well as light alkali and earth alkaline metals Li, Na, Be, Mg, and Ca for their suitability as possible codopants of donors in heavily doped Si. The objective was to determine, by virtue of *ab initio* simulations on the atomistic level, if any of these impurities can, to some extent, preclude the percolation, clustering, and hence the electrical deactivation of donors at high concentrations. The codopants were studied with regard to their tendency to (a) form pairs with one another and with the donors, and (b) to annihilate vacancies, the main n -type killer defects, present in various donor-vacancy clusters. Moreover, we determined the electrical behavior of the relevant impurity defects involving donors and codopants. Both C and Ge were found to bind too weakly to any donor in Si. In addition, C stabilizes the shallow donor electrons of P, As, and Sb when sharing neighboring lattice positions. Due to their small ionic radius, group I and II elements are likely to annihilate lattice vacancies surrounded by donor atoms. Having only one valence s electron, however, the alkali metals are less efficient in reactivating donor-vacancy clusters than the earth alkalines Be, Mg, and Ca. The most promising candidate for the codoping with P, As, and Sb is Mg, which in addition exhibits a lower ionization potential for its valence s electrons in Si than Be and, therefore, in almost any complex configuration shows a stronger tendency to act as a donor.

*Corresponding author. Fax: +41-1-632-11-94.

¹K. C. Pandey, A. Erbil, G. S. Cargill III, R. F. Boehme, and D. Vanderbilt, Phys. Rev. Lett. **61**, 1282 (1988).

²M. Ramamoorthy and S. T. Pantelides, Phys. Rev. Lett. **76**, 4753 (1996).

³M. A. Berding, A. Sher, and M. van Schilfgaarde, Appl. Phys. Lett. **72**, 1492 (1998).

⁴S. Solmi, M. Attari, and D. Nobili, Appl. Phys. Lett. **80**, 4774 (2002).

⁵Y. Takamura, P. B. Griffin, and J. D. Plummer, J. Appl. Phys. **92**, 235 (2002).

⁶P. M. Voyles, D. A. Muller, J. L. Grazul, P. H. Citrin, and H-J. L. Gossmann, Nature (London) **416**, 826 (2002).

⁷V. Ranki, J. Nissilä, and K. Saarinen, Phys. Rev. Lett. **88**, 105506 (2002).

⁸P. A. Packan, Science **285**, 2079 (1999).

⁹H. Katayama-Yoshida, T. Nishimatsu, T. Yamamoto, and N. Orita, J. Phys.: Condens. Matter **13**, 8901 (2001).

¹⁰S-H. Wei, Comput. Mater. Sci. **30**, 337 (2004).

¹¹V. Moroz, Y. S. Oh, D. Pramanik, H. Graoui, and M. A. Foad, Appl. Phys. Lett. **87**, 051908 (2005).

¹²A. Zunger, Appl. Phys. Lett. **83**, 57 (2003).

¹³D. C. Mueller, E. Alonso, and W. Fichtner, Phys. Rev. B **68**, 045208 (2003).

¹⁴M. Rummukainen, I. Makkonen, V. Ranki, M. J. Puska, K. Saarinen, and H-J. L. Gossmann, Phys. Rev. Lett. **94**, 165501

- (2005).
- ¹⁵G. Kresse and J. Hafner, Phys. Rev. B **47**, R558 (1993).
- ¹⁶G. Kresse and J. Furthmüller, Comput. Mater. Sci. **6**, 15 (1996).
- ¹⁷G. Kresse and D. Joubert, Phys. Rev. B **59**, 1758 (1999).
- ¹⁸H. J. Monkhorst and J. D. Pack, Phys. Rev. B **13**, 5188 (1976).
- ¹⁹D. C. Mueller and W. Fichtner, Phys. Rev. B **70**, 245207 (2004).
- ²⁰V. Ranki, K. Saarinen, J. Fage-Pedersen, J. L. Hansen, and A. N. Larsen, Phys. Rev. B **67**, 041201(R) (2003).
- ²¹M. O. Henry, E. C. Lightowers, N. Killoran, D. J. Dunstan, and B. C. Cavenett, J. Phys. C **14**, L255 (1981).
- ²²V. Ranki and K. Saarinen, Phys. Rev. Lett. **93**, 255502 (2004).
- ²³C. S. Fuller and J. A. Ditzenberger, Phys. Rev. **91**, 193 (1953).
- ²⁴J. C. Larue, Phys. Status Solidi A **6**, 143 (1971).
- ²⁵G. L. Miller and W. A. Orr, Appl. Phys. Lett. **37**, 1100 (1980).
- ²⁶E. M. Pell, Phys. Rev. **119**, 1222 (1961).
- ²⁷E. Tarnow, S. B. Zhang, K. J. Chang, and D. J. Chadi, Phys. Rev. B **42**, 11252 (1990).
- ²⁸See, for instance, Ref. 13 and references therein.
- ²⁹If the “codopant” is a Si atom, this binding energy obviously corresponds to the negative energy of a Frenkel pair generation in the proximity of 0–4 arsenic atoms.
- ³⁰Yet, at annealing temperatures, this energy barrier will not prevent the reverse reaction of Si interstitial ejection from taking place, as can be observed experimentally in highly As-doped samples.
- ³¹The codopants occupy two nearest tetrahedral interstitial sites.
- ³²In *p*-type Si, also the Be_s-Be_i pair, like the Mg_s-Mg_i pair, would be electrically neutral, in accordance with the findings of Tarnow *et al.* (See Ref. 27).
- ³³A. G. Milnes, *Deep Impurities in Semiconductors* (Wiley, New York, 1973).
- ³⁴E. Otha and M. Sakata, Solid-State Electron. **22**, 677 (1978).